

Determination of phosphorylation and deprotonation induced higher order structural transitions in α_s -caseins

Ilokugbe Ettah and Lorna Ashton*

Department of Chemistry, Lancaster University, Lancaster, Lancashire LA1 4YB, UK

* Correspondence: l.ashton@lancaster.ac.uk

Abstract

One extremely sensitive and highly successful application of Raman spectroscopy is the structural characterisation of proteins. Understanding higher order structure and its effect on protein stability is essential not only for biopharmaceutical and food manufacturing but also for the understanding of diseases that result from the misfolding of proteins including diabetes type II, Alzheimer's and Parkinson's disease. Due to the large amount of structural information available in Raman spectra, even small alterations in protein conformations including increased exposure of binding regions or changes in geometry of secondary structural elements can be identified. In this study, we demonstrate the unique sensitivity of Raman spectroscopy to subtle structural transitions in an intrinsically open, flexible protein, α_s -casein, in response to phosphorylation and deprotonation. Through the application of 2D correlation analysis two separate transition phases have been identified from pH 6-9 and pH 10-12 for both phosphorylated and dephosphorylated α_s -casein. However, the actual structural changes observed in each pH range differed considerably between the phosphorylated and dephosphorylated α_s -casein. Furthermore, the presence of the phosphorylated serine residues is demonstrated to have a shielding effect during deprotonation of the protein.

Proteins, including enzymes, antibodies and transport molecules, are not only essential for maintaining health, but also play an important role in biopharmaceutical and food manufacture. However, regardless of the role they play proteins will only function optimally when in the correct structural conformation and devastating effects can occur as a result of protein misfolding, for example diseases such as Alzheimer's, Parkinson's, diabetes Type II and atherosclerosis all result from misfolded proteins forming amyloid fibril plaques.¹ Maintaining the correct fold is also essential for protein based therapeutics and in food manufacturing if protein activity is to be preserved throughout production and storage.²⁻⁴ Even small changes in conformation that occur as a result of post-translational modifications (PTM) and variations in preparation and formulation, including pH, can affect protein stability and function. Consequently, there is a need for analytical methods that can identify subtle changes in conformation and stability throughout the manufacturing processes. Raman spectroscopy provides an ideal analytical tool to assess changes in the higher order structure and stability of proteins. The technique is non-destructive, rapid, can be applied to low and high concentrations of samples and as water is a weak Raman scatterer it can be applied to proteins in aqueous conditions.

Phosphorylation is an important PTM, which effects protein conformation and stability. The phosphorylation of a protein by a kinase, or dephosphorylation by a phosphatase can play an essential role in cellular processes.^{5,6} In particular, the heavily phosphorylated casein proteins, act as both storage and transport molecules for calcium in the mammary glands but also act as protecting agents against amyloid formation during self-association of individual caseins.⁷⁻⁹ Due to the difficulties in crystallising caseins they were all initially thought of as random coil or intrinsically denatured proteins, however, a range of spectroscopic studies have identified the presence of secondary structural elements including α -helix, β -sheet, turns, and polyproline II (PP-II) confirmation, although the exact percentage content of each is still to be unequivocally determined.^{7, 9-12} Despite the existence of such structural elements, caseins do not form globular conformations but remain in more open and flexible forms.^{7,9} This open and more flexible structure of caseins compared to other proteins is attributed to the high content of proline residues and high surface hydrophobicity^{7, 8, 11} and whilst this offers some flexibility in the protein conformation maintaining protein stability and the correct fold is still essential for protein function. Studies of the individual caseins suggest that α_{s1} - and β -casein play an important role in preventing protein misfolding and amyloid formation in α_{s2} - and κ -caseins, respectively, during self-assembly and aggregation in the absence of calcium.⁷⁻⁹ In this study, we have compared pH-induced structural changes in bovine α_s -casein (a mix of the two α_{s1} - and α_{s2} - components at a 4:1 ratio in bovine milk) in both the phosphorylated and dephosphorylated forms to investigate important changes in protein conformation that result from deprotonation and phosphorylation using Raman spectroscopy and 2D correlation analysis.

Experimental

Data collection

Samples of phosphorylated and dephosphorylated α_s -casein from bovine milk were purchased from Sigma Aldrich and used without further purification. Separate samples were prepared at different pH's in the pH range 5.7 to 12.3 at concentrations of 10 mg/mL, to ensure full deprotonation of the

protein. The dry material was dissolved in deionised water and pH was adjusted using dilute NaOH or HCl. The pH of each sample was measured using a pH meter (HI2210) by Hanna Instruments (± 0.5). For the phosphorylated α_s -casein sample pH values of 5.7, 6.5, 7.7, 8.7, 9.2, 10.2, 11.1 and 12.1 were recorded and for the dephosphorylated α_s -casein pH values of 6.1, 7.0, 7.6, 8.9, 10.1, 11.7 and 12.3 were recorded. Native samples (samples without any adjustment of pH) were recorded at pH 6.5 for phosphorylated α_s -casein and pH 7.0 for dephosphorylated α_s -casein. 400 μ L of each solution was pipetted into a quartz 96-well plate before spectral collection. All Raman measurements were performed using a confocal Raman system (inVia, Renishaw plc, Wotton-Under Edge, UK) coupled to a 785 nm wavelength laser, x15 objective and 1200 mm grating. Spectra were acquired for 10s exposure with 180 accumulations (total collection time 30 minutes) with a laser power at sample of ~ 30 mW. 3 repeat spectra were collected for each pH and then averaged for data analysis.

2D correlation spectroscopy (2DCOS)

2DCOS is a cross-correlation technique, which can be applied to a set of perturbation-induced spectra as a function of two independent wavenumber positions. The acquired data set (ordered in the direction of relatively consistent perturbation-induced changes) forms an experimental matrix to which the cross-correlation function is applied resulting in a new set of matrices improving visualization and therefore interpretation of the spectral variations.^{4, 13, 14} Synchronous matrices identify similarities in behaviour, whilst asynchronous matrices identify differences in behaviour between data points at two independent wavenumbers. Autocorrelation plots display significantly varying peak intensities (identified in the synchronous matrix) from which the overall extent of intensity changes of individual bands can be determined and compared. Perturbation correlation moving windows (PCMW) matrices relate the spectral variations to the specific perturbation values identifying distinct phases in behaviour.^{4, 13, 14}

As has been extensively discussed in previous papers, appropriate data preprocessing is necessary to generate reliable and clear 2DCOS plots, particularly with biological samples.^{15, 16} For the Raman spectra presented here solvent extraction, normalisation to the intensity invariant Raman band measured at ~ 1450 cm^{-1} (arising from methylene deformations), baseline subtraction and smoothing were all carried out in MATLAB software (version R2016a) using an in-house toolbox. Interpolation was also applied to the 2DCOS data sets before calculation of 2DCOS matrices. Full details of all data processing approaches are available in Supplementary Information).

Results and Discussion

Comparison of phosphorylated and dephosphorylated α_s -casein

Figure 1 compares the Raman spectra of the phosphorylated and dephosphorylated forms of α_s -casein where numerous Raman features assigned to amino acid residues and secondary structure can clearly be observed (Table 1). As previously reported by Jarvis et al.¹⁷ who successfully quantified casein phosphorylation using Raman spectroscopy, the two spectra are very similar with only minimal intensity differences between the phosphorylated and dephosphorylated forms of α_s -casein. In Figure 1 the bands assigned to side chain residues at 1003 cm^{-1} (Phe),^{18, 19} $850/830$ cm^{-1}

(Tyr Fermi Doublet)^{20, 21} and 755 cm⁻¹ (Trp)^{22, 23} as well as bands assigned to secondary structure at 1667 cm⁻¹ (β -sheet),²⁴ 1337 cm⁻¹ (α -helix / Trp),^{25, 26} 1318 cm⁻¹ (α -helix)^{15, 26} and 1250 cm⁻¹ (disordered)^{15, 27} can all be observed to have a slightly higher intensity in the phosphorylated spectrum compared to the dephosphorylated spectrum. The decrease in Raman spectral intensity has previously been attributed to a loss of structure and a change in solvent exposure of the aromatic amino acids.^{17, 28} In particular, the significant difference in intensity and bandwidth at 1003 cm⁻¹ was identified as an important feature in the calibration method used to quantify phosphorylation.¹⁷

However, previous studies using CD and fluorescence spectroscopy to measure secondary structural differences between phosphorylated and dephosphorylated α_s -casein could not identify any differences in secondary structure and in fact an increase in secondary structure in the dephosphorylated form has also been suggested.⁸ Raman bands can arise specifically from side chain orientation as well as the quantity of amino acids and secondary structure and therefore changes observed in the Tyr and Trp Raman bands at 755, 850/830 and 1337 cm⁻¹ can be associated with changes in side chain orientation and/or solvent exposure (Table 1). Variations in the wavenumber position of α -helical assigned bands in the region of 1315-1345 cm⁻¹ have also been associated with subtle changes in α -helical symmetry²⁵ and again, it may be these changes rather than a distinctive loss of secondary structure that is being detected by the spectral variations observed in Figure 1. Importantly, in Figure 1 there are several Raman bands with the same intensity and position regardless of whether α_s -casein is phosphorylated or not including Raman bands observed at 1615, 1208, 1173, 1124 and 930 cm⁻¹.

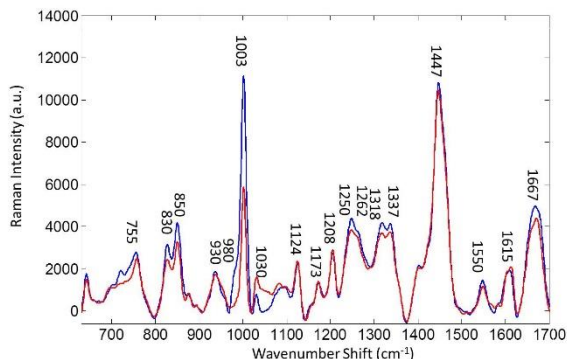


Figure 1. Averaged (n=3) Raman spectra of phosphorylated α_s -casein (blue) and dephosphorylated α_s -casein (red). Further information on band assignments is provided in Table 1.

Table 1. Proposed Raman band assignments for phosphorylated and dephosphorylated α_s -casein

Wavenumber	Proposed Assignment
1667 cm ⁻¹	β -sheet ²⁴
1615-1600 cm ⁻¹	Tyr, downward shift with protonation, minor contribution from Phe ^{21, 29, 30}
1575 cm ⁻¹	Tyr ²¹
1550 cm ⁻¹	Trp ^{18, 22}
1460 cm ⁻¹	Side chains, Ala, Leu ³¹
1447 cm ⁻¹	CH ₂ def ^{15, 32}
1400-1415 cm ⁻¹	Carboxyl stretch, ionization state ^{15, 29, 30}

1337 cm ⁻¹	Trp ²⁶ α -helix ²⁵
1318 cm ⁻¹	α -helix ^{15, 25}
1262 cm ⁻¹	α -helix ^{26, 29}
1250 cm ⁻¹	Disordered structure ^{15, 27}
1234 cm ⁻¹	β -sheet ²⁴
1208 cm ⁻¹	Tyr ^{21, 32}
1173 cm ⁻¹	Tyr ^{21, 32}
1124 cm ⁻¹	Trp ³²
1065 cm ⁻¹	C-C stretch, Charged side chains Lys, Asp and Glu ^{32, 33}
1030 cm ⁻¹	Phe ^{19, 32}
1003 cm ⁻¹	Phe ^{18, 19}
980 cm ⁻¹	Phosphate stretch ^{17, 28, 34}
930 cm ⁻¹	α -helix ^{15, 24}
850 cm ⁻¹	Tyr, in-plane ring-breathing motion ^{20, 21}
830 cm ⁻¹	Tyr, C-H out of plane bending ^{20, 21}
755 cm ⁻¹	Trp, indole ring ^{18, 24}

With the exception of the band observed at 930 cm⁻¹ these invariant bands are assigned to Tyr and Trp residues reflecting that the numbers of specific residues remain consistent between phosphorylated and dephosphorylated forms of α_s -casein reported as 10 and 2 for bovine α_{s1} -casein and 11 and 2 for bovine α_{s2} -casein, respectively.^{7, 35} The band at 930 cm⁻¹ is assigned to α -helix content and has not been shown to change with variations in α -helix symmetry¹⁵ also suggesting that while the overall secondary structure content of α_s -casein remains consistent regardless of phosphorylation subtle changes in conformation can be determined. Interestingly, the Raman band at 1003 cm⁻¹ assigned to Phe displays the largest difference in intensity in Figure 1 despite this peak often being assigned as invariant to conformation changes and being used for normalisation of biomolecular spectra, although more recent studies suggest that changes in intensity are associated with variations in interactions and backbone orientation around the Phe residues.^{18, 19} As previously stated Jarvis et al.¹⁷ determined that the Raman band at 1003 cm⁻¹ was the largest contributing peak in the quantification of phosphorylated to dephosphorylated α_s -casein ratios. There is a difference in the number of Phe residues in bovine α_{s1} -casein (n=8) and α_{s2} -casein (n=5) which may differ slightly in ratio in the phosphorylated and dephosphorylated α_s -casein samples available from Sigma Aldrich as exact α_{s1} -casein: α_{s2} -casein ratios are not determined although in bovine milk this is reported as a 4:1 ratio. The importance of the Raman band at 1003 cm⁻¹ for quantification of phosphorylation may also be a result of its proximity to the 980 cm⁻¹ phosphate stretch band (discussed below) which is observed as a shoulder in Raman spectrum of phosphorylated α_s -casein.

The challenge of observing phosphate peaks in proteins is well documented and has previously been accredited to the presence of overlapping peptide bands in the same region as well as the lower solubility of phosphorylated proteins in aqueous solution compared to phosphorylated amino acids.^{17, 36} However, in a previous study we successfully demonstrated that the presence of phosphate peaks at ~980 and 1080 cm⁻¹ in Raman spectra of amino acids and proteins is very much pH dependent.²⁸ In Figure 1 a shoulder at ~980 cm⁻¹ can be observed for phosphorylated α_s -casein at a native pH 7 whose increasing intensity is associated with the number of phosphorylated monomers in a dibasic form (-OPO₃²⁻) where the negative charge is delocalized over the three oxygen atoms.^{5, 28, 34} The phosphate peak at ~1080 cm⁻¹ is associated with the monobasic form (-

OPO₃H⁻) and therefore increases in intensity with increasingly acidic conditions. Only once highly acidic conditions (pH<2) are reached does stabilization of the fully protonated structure occur (-OPO₃H₂).^{5, 28, 36} Examined closely the spectra in Figure 1 do reveal a slightly broader peak at ~1080 cm⁻¹ in the phosphorylated compared to the dephosphorylated form of α_s -casein, which may be associated with a monobasic phosphate stretch. However, the feature is too small to be conclusive without further investigation and is not observed in the averaged spectrum measured at pH 5.7 (Figure 2b).

Phosphorylated α_s -casein 2DCOS autocorrelation

As previously discussed the presence or absence of PTMs as well as protein protonation can significantly affect protein stability, therefore to gain a better understanding of α_s -casein in the different forms we carried out 2DCOS on pH dependent spectral data. Figure 2 displays the pH-induced spectral data set of phosphorylated α_s -casein alongside the 2DCOS autocorrelation revealing numerous spectral variations dominated by side chain and secondary structure assigned bands (Table 1). One of the challenges when analysing spectral data sets of induced transitions in proteins is determining the most important variations from what are often very complex and detailed spectra. By calculating the 2DCOS autocorrelation (Figure 2a) not only can the most significantly changing bands be identified but also the extent of variation can be directly compared across peaks.^{13, 37}

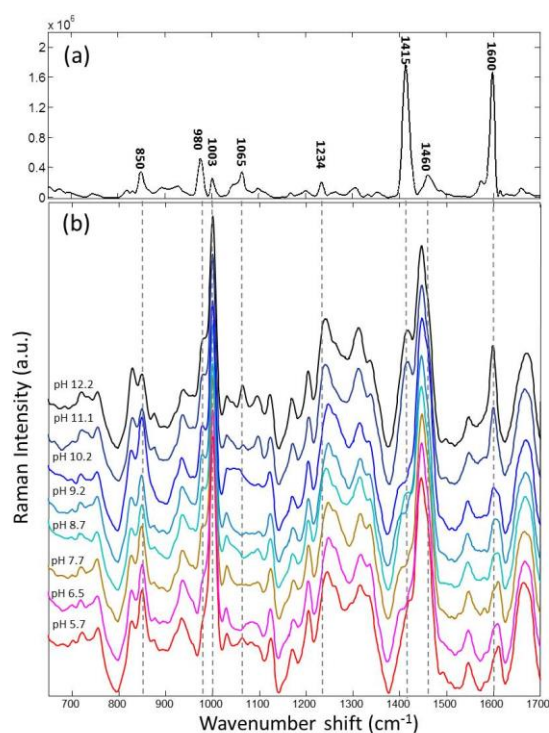


Figure 2. pH-induced spectral variations of phosphorylated α_s -casein. (a) 2DCOS autocorrelation and (b) phosphorylated α_s -casein spectra acquired at solvent pH 5.7, 6.5, 7.7, 8.7, 9.2, 10.2, 11.1 and 12.2.

From the intensity of the autocorrelation peaks in Figure 2a the largest spectral variations with changing solvent pH can be determined to occur at ~ 1415 and 1600 cm^{-1} followed by the peak at 980 cm^{-1} for phosphorylated α_s -casein. As expected the shoulder at 980 cm^{-1} can be observed to increase with increasing pH monitoring a change from mixed monobasic and dibasic phosphate populations to the dibasic form only.^{28,36} The Raman band at 1600 cm^{-1} is assigned to Tyr and Phe and more specifically to the deprotonation of Tyr residues whilst the 1415 cm^{-1} band is assigned to ionised carboxylic acid side chains (Table 1) and therefore also expected to vary in intensity as solvent pH is altered. A significant increase in intensity for both bands can be observed at pH 11.1 and 12.2 compared to the lower pH values (Figure 2b). The pK_a value for Tyr is reported to be 10.3 ± 1.2 and the dramatic increase in intensity at 1600 cm^{-1} above pH 10 can be attributed to the deprotonation of Tyr residues.^{21,30} An additional peak in Figure 2b can also be observed at 1615 cm^{-1} below pH 10 which disappears with increased intensity at 1600 cm^{-1} . A shift from 1616 to 1600 cm^{-1} has previously been reported in Raman spectra of Tyr with increasing pH.^{21,30} The band at $\sim 1065\text{ cm}^{-1}$ is also assigned to changes in charged of amino acids³² and although the autocorrelation peak at 1065 cm^{-1} has low intensity compared to the peaks at 1415 and 1600 cm^{-1} the presence of distinct autocorrelation peaks does indicate a significant pH-induced intensity change with deprotonation of phosphorylated α_s -casein.

Phosphorylated α -casein PCMW

While the autocorrelation provides useful information as to which bands vary in intensity with changing conditions it does not directly relate these spectral changes to the actual perturbation. The further 2DCOS technique PCMW overcomes this problem by directly relating the spectral transitions.^{13,14,38} Figure 3 displays PCMW contour plots of the pH-induced phosphorylated α_s -casein plotted as a function of spectral wavenumber and the average translating perturbation, in this case pH. In Figure 3 the largest increases in intensity (identified by the darker colour and larger number of contours) can be observed for Raman bands at 1415 and 1600 cm^{-1} from pH 10-12. These are consistent with the changes previously identified from the autocorrelation and the spectra (Figure 2). However, in the PCMW contours indicate an increase in intensity only from \sim pH 8.3-10 for the peak at 1600 cm^{-1} , whereas for the peak 1415 cm^{-1} fluctuations in intensity occur throughout the full pH range. In Figure 3 a positive (red) contour at 980 cm^{-1} can be observed from pH 5.7-9 indicating the increase in the phosphate stretch assigned peak with increasing pH, however, no contours and therefore no further significant spectral changes are determined above pH 9. This lack of contours suggests that all phosphates are dibasic, with the negative charge delocalised over the three oxygen atoms at pH 9.

From a general overview of the PCMW shown in Figure 3 there appears to be two transition phases as a result of increasing pH, and initial phase from pH $\sim 5.7-9$ and a second from pH $\sim 10-12$. Although contours are observed between pH 9-10 only one spectrum was recorded in this pH range and therefore these contours may be a result of small fluctuations between individual spectra, as can be seen for the Raman bands at 1065 and 1460 cm^{-1} in the spectra and further data at smaller pH steps are needed to confirm this potential transition phase. These fluctuations may also account for why a negative contour is observed from pH 10.5-11.5 for the Raman band at 1065 cm^{-1} in Figure 3 despite the fact the appearance, and therefore increase in intensity, of a distinct peak can be observed in the Raman spectra (Figure 2b).

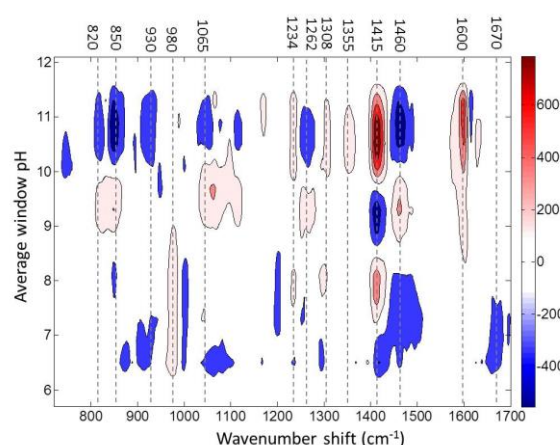


Figure 3. PCMW of pH-induced phosphorylated α_s -casein spectral data. PCMW plotted as a function of spectral wavenumber and average translating window pH. Contours shaded red indicate Raman bands that are increasing in intensity with increasing pH, while blue shading indicates decreasing peak intensity with increasing pH. The darker the shade of blue or red and the closer together the contours the greater the change in intensity, as indicated by the colour shading bar. The scale on this bar is of arbitrary units. A moving window size of 5 with a maximum of 6 contours was applied.

Despite the influence of these minor fluctuations, the lack of intensity variation in the phosphate stretch at 980 cm^{-1} and the increased number of contours in the second transition range compared to the first indicates that very different conformational changes occur from pH 6-9, compared to those that occur from pH 10-12, most likely as a result of the phosphorylated serine molecules providing protection from deprotonation of other charged side chain residues. In particular, from pH 10-12 decreases in intensity associated with changes in side chain environment can be determined from negative (blue) contours observed at 820, 850, 1065 and 1460 cm^{-1} . Furthermore, decreases in Raman band intensity can also be identified from contours centred at ~ 930 and 1262 cm^{-1} both assigned to α -helix and therefore indicating a loss of α -helix at this pH range. Two positive contours can also be observed at 1308 and 1355 cm^{-1} despite the fact that Raman bands assigned to α -helix are actually observed at 1318 and 1337 cm^{-1} (Figure 1 and 2b). In 2DCOS the most significantly changing wavenumbers do not always match to the maximum band intensity as the correlation determines the largest spectral changes which can occur as a result of shoulders and/or broadening as well as changes in maximum peak intensity.¹⁵ In Figure 2b an increase in the peak at 1318 cm^{-1} can be observed and the two contours observed at 1308 and 1355 cm^{-1} in the PCMW (Figure 3) could potentially indicate a broadening of this wavenumber region suggesting a change in α -helical structure.

Distinctive Raman bands assigned to β -structure in protein spectra are frequently observed in the regions of 1665-1670 and $1230\text{-}1245\text{ cm}^{-1}$. In Figure 3 a negative contour can be observed from pH 6-8 that shifts centrally from 1660 to 1670 cm^{-1} . This upward shift is reported to indicate an increase in less ordered β -structure/ β -turns, including the possible increase in PPII structure³⁰ suggesting conformational transitions from β -sheet to β -turn or less defined structure alongside an overall

decrease in the total amount of β -structure with deprotonation of the phosphate serine groups. No further contours are observed in the region of 1665-1670 cm^{-1} with increasing pH although surprisingly a positive contour can be observed at 1234 cm^{-1} also assigned to β -sheet potentially suggesting an increase in β -sheet. Only a loss in secondary structure, not an increase, is expected to occur with deprotonation as increasing alkalinity has been reported to result in the unfolding / denaturing of casein proteins and no self-assembly or aggregation has been observed.^{11, 39} However, when examined closely in Figure 2b (and Figure 1) it can be determined that a Raman band is observed at 1250 cm^{-1} and it may be a broadening of the 1250 cm^{-1} band that produces the contour observed at 1234 cm^{-1} . The Raman band at 1250 cm^{-1} is assigned to disordered structure^{15, 27} and therefore an increase in intensity would be consistent with the loss of a helical and β -structure as a result of increasing pH.

Dephosphorylated α -casein autocorrelation and PCMW

Figure 4 displays the pH-induced spectral data set of dephosphorylated α_s -casein alongside the 2DCOS autocorrelation. As with the previously discussed autocorrelation (Figure 2a) spectral variations dominated by side chain assigned bands can be observed for the dephosphorylated α_s -casein but relative intensities differ considerably. Whilst the peaks at 1415 and 1600 cm^{-1} assigned to side chain protonation still dominate in Figure 4a the peak at 1065 cm^{-1} is also very intense possibly suggesting increased deprotonation of Lys, Asp and Glu side chains in dephosphorylated compared to phosphorylated α_s -casein. As expected, the autocorrelation peak at 980 cm^{-1} assigned to the dibasic phosphate stretch is no longer observed. In the PCMW of the pH-induced dephosphorylated α_s -casein spectral data set (Figure 5) the wavenumber position of the contours is again similar to that of the phosphorylated α_s -casein PCMW (Figure 3) but the actual position of contours with respect to pH is significantly different. Unlike the phosphorylated α_s -casein, the PCMW of the dephosphorylated form has the largest number of contours in the pH range 6-9. In fact, the pattern and position of contours in this lower pH range in Figure 5 appears similar to the contour patterns in the pH range 10-12 in the phosphorylated form in Figure 3 indicating that side chain deprotonation occurs at a lower pH in the absence of phosphate. The contours observed at 1415 cm^{-1} again vary in colour as pH is increased indicating an initial increase then decrease before a further increase in intensity.

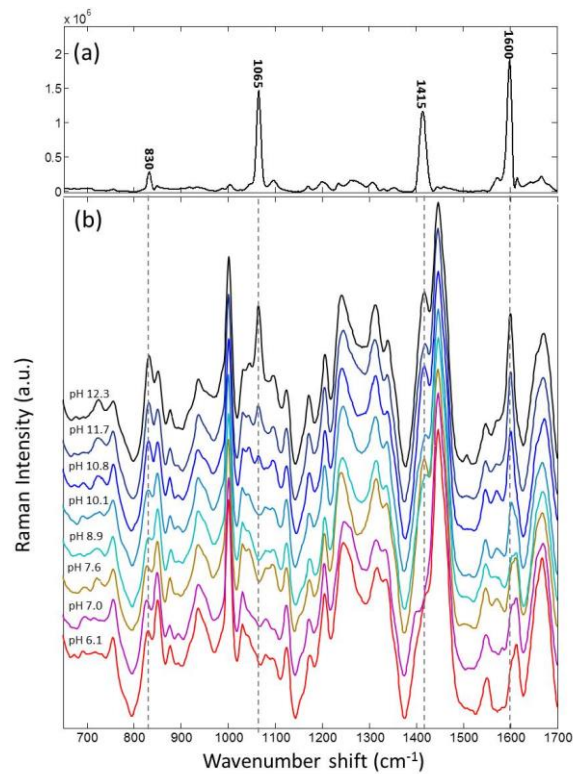


Figure 4. pH-induced spectral variations of dephosphorylated α_s -casein. (a) 2DCOS autocorrelation and (b) phosphorylated α_s -casein spectra acquired at solvent pH 6.1, 7.0, 7.6, 8.9, 10.1, 10.8, 11.7 and 12.3

The PCMW plots (Figure 3 and 5) demonstrate the sensitivity of Raman spectroscopy combined with 2DCOS for determining even subtle structural changes in protein stability as a result of protonation and PTM. As previously discussed, in both forms of α_s -casein the deprotonation of side chain molecules can clearly be determined with increasing pH, however this occurs at a much lower pH (pH 6-9) in the dephosphorylated α_s -casein compared to the phosphorylated α_s -casein where changes are observed from pH 9-12. This shielding effect of the additional phosphate groups may also influence the loss of α -helical structure indicated by intensity changes in the Raman bands in the region of 1308-1355 cm^{-1} and at 1262 cm^{-1} which also occur at a lower pH in the dephosphorylated α_s -casein compared to phosphorylated. Interestingly, the α -helical Raman band at 930 cm^{-1} can be observed to decrease in intensity across the full pH range for both forms of α_s -casein and therefore this loss of secondary structure occurs regardless of phosphate deprotonation. Further Raman bands where the response to increasing pH is not affected by changes in phosphorylation include bands observed at 1003 cm^{-1} , 1308 cm^{-1} , 1600 cm^{-1} , and 1670 cm^{-1} .

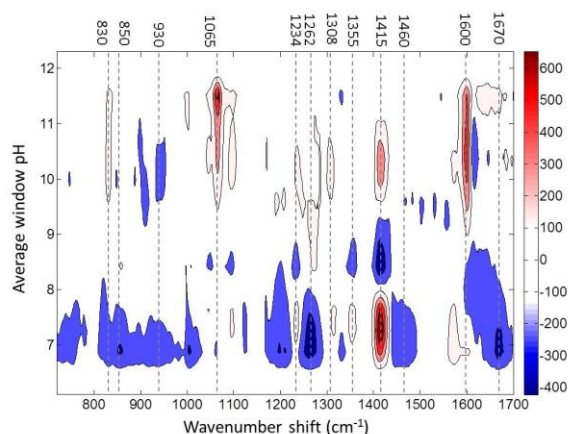


Figure 5. PCMW of pH-induced dephosphorylated α_5 -casein spectral data. PCMW plotted as a function of spectral wavenumber and average translating window pH. Contours shaded red indicate Raman bands that are increasing in intensity with increasing pH, while blue shading indicates decreasing peak intensity with increasing pH. The darker the shade of blue or red and the closer together the contours the greater the change in intensity, as indicated by the colour shading bar. The scale on this bar is of arbitrary units. A moving window size of 5 with a maximum of 6 contours was applied.

A further interesting difference in response to increasing pH of the phosphorylated compared to the dephosphorylated α_5 -casein is observed in the well-established Tyr Fermi Doublet, a known marker of hydration and solvent exposure of Tyr residues.^{20, 21} A decrease in the calculated ratio of peak intensities recorded at 830 and 850 cm^{-1} (I_{850} / I_{830}) is associated with a decrease in solvent exposure. For both the phosphorylated and dephosphorylated spectral data presented in this study a decrease in the I_{850} / I_{830} ratio was observed to decrease from ~ 1.5 to 0.9 in both experiments with increasing pH. However, when the spectra and 2DCOS results are examined closely very different behaviour is observed for each peak. For phosphorylated α_5 -casein an autocorrelation peak can only be observed at 850 cm^{-1} (Figure 2a) which can be observed in the spectral data to increase in intensity at pH 10.2 but to decrease at pH 12.2 compared to the more acidic pH range, no obvious variations can be observed for the 830 cm^{-1} Raman band (Figure 2b). In contrast in the dephosphorylated α_5 -casein autocorrelation a peak is only observed at 830 cm^{-1} and a clear increase in Raman intensity is observed in the spectra with increasing pH (Figure 4). The increase in intensity of the Raman band at 830 cm^{-1} from pH 9 and 12 can also be clearly determined in the PCMW (Figure 5) where a positive contour is observed. No contours are observed for the peak at 850 cm^{-1} in this pH range although a negative contour is observed from pH 6-8. A detailed investigation of Raman markers of tyrosine by Hernández et al.²¹ suggests that the two bands arise from different vibrational modes, with variations in intensity of the 850 cm^{-1} band arising from in-plane ring breathing modes whereas 830 cm^{-1} corresponds to the out-of-plane C-H bond collective motions. Consequently, it may be this very specific difference in vibrational mode of that accounts for the difference in Tyr spectral variations observed between pH-induced changes phosphorylated and dephosphorylated α_5 -casein.

Conclusion

In this study we have demonstrated the unique sensitivity of Raman spectroscopy for the determination of even the most subtle of changes in protein conformation as a result of phosphorylation and deprotonation. While there is a limit to the extent of structural information that be gained from a single Raman spectrum of a protein we have shown how, vast amounts of information can be gained by comparing perturbation-induced variations in Raman spectra. By combining Raman spectroscopy with 2DCOS more detailed analysis of protein stability during bioprocessing and food manufacturing can be achieved. .

Acknowledgments

This research was funded by the EPSRC Centre for Doctoral Training in Emergent Macromolecular Therapies. The authors would like to thank the EPSRC Centre for Innovative Manufacturing in Emergent Macromolecular Therapies and Paul Dalby in the Department of Biochemical Engineering, University Collage, London for their support.

Supporting Information.

Data Processing

Water Subtraction

Normalisation

2D Correlation Interpolation

2D Calculations and PCMW

References

1. Cremades, N.; Dobson, C. M., The contribution of biophysical and structural studies of protein self-assembly to the design of therapeutic strategies for amyloid diseases. *Neurobiol. Dis.* **2018**, *109*, 178-190.
2. Lauer, T. M.; Agrawal, N. J.; Chennamsetty, N.; Egodage, K.; Helk, B.; Trout, B. L., Developability index: A rapid in silico tool for the screening of antibody aggregation propensity. *Journal of Pharmaceutical Sciences* **2012**, *101* (1), 102-115.
3. Obrezanova, O.; Arnell, A.; de la Cuesta, R. G.; Berthelot, M. E.; Gallagher, T. R. A.; Zurdo, J.; Stallwood, Y., Aggregation risk prediction for antibodies and its application to biotherapeutic development. *Mabs* **2015**, *7* (2), 352-363.
4. de la Cuesta, R. G.; Goodacre, R.; Ashton, L., Monitoring Antibody Aggregation in Early Drug Development Using Raman Spectroscopy and Perturbation-Correlation Moving Windows. *Analytical Chemistry* **2014**, *86* (22), 11133-11140.
5. Wojciechowski, M.; Grycuk, T.; Antosiewicz, J. M.; Lesyng, B., Prediction of secondary ionization of the phosphate group in phosphotyrosine peptides. *Biophys. J.* **2003**, *84* (2), 750-756.
6. Denu, J. M.; Stuckey, J. A.; Saper, M. A.; Dixon, J. E., Form and function in protein dephosphorylation. *Cell* **1996**, *87* (3), 361-364.
7. Farrell, H. M.; Brown, E. M.; Malin, E. I., In *Advanced dairy chemistry. Protein Vol 1, Basic Aspects*, 4th ed.; Springer Science & Business Media: New York, 2013; pp 84-161.
8. Koudelka, T.; Hoffmann, P.; Carver, J. A., Dephosphorylation of alpha(s)- and beta-Caseins and Its Effect on Chaperone Activity: A Structural and Functional Investigation. *J. Agric. Food Chem.* **2009**, *57* (13), 5956-5964.

9. Holt, C.; Carver, J. A.; Ecroyd, H.; Thorn, D. C., Invited review: Caseins and the casein micelle: Their biological functions, structures, and behavior in foods. *J. Dairy Sci.* **2013**, *96* (10), 6127-6146.
10. Farrell, H. M.; Malin, E. L.; Brown, E. M.; Mora-Gutierrez, A., Review of the chemistry of alpha(S2)-casein and the generation of a homologous molecular model to explain its properties. *J. Dairy Sci.* **2009**, *92* (4), 1338-1353.
11. Tauzin, J.; Miclo, L.; Roth, S.; Molle, D.; Gaillard, J. L., Tryptic hydrolysis of bovine alpha(S2)-casein: identification and release kinetics of peptides. *Int. Dairy J.* **2003**, *13* (1), 15-27.
12. Smyth, E.; Syme, C. D.; Blanch, E. W.; Hecht, L.; Vasak, M.; Barron, L. D., Solution structure of native proteins with irregular folds from Raman optical activity. *Biopolymers* **2001**, *58* (2), 138-151.
13. Noda, I.; Ozaki, Y., *Two-dimensional correlation spectroscopy: applications in vibrational and optical spectroscopy*. John Wiley & Sons: 2005.
14. Noda, I., Vibrational two-dimensional correlation spectroscopy (2DCOS) study of proteins. *Spectroc. Acta Pt. A-Molec. Biomolec. Spectr.* **2017**, *187*, 119-129.
15. Ashton, L.; Barron, L. D.; Hecht, L.; Hyde, J.; Blanch, E. W., Two-dimensional Raman and Raman optical activity correlation analysis of the α -helix-to-disordered transition in poly(L-glutamic acid). *Analyst* **2007**, *132* (5), 468-479.
16. Ashton, L.; Boguslawa, C. M. B.; Blanch, E. W., Application of two-dimensional correlation analysis to Raman optical activity. *Journal of Molecular Structure* **2006**, *799* (1-3), 61-71.
17. Jarvis, R. M.; Blanch, E. W.; Golovanov, A. P.; Screen, J.; Goodacre, R., Quantification of casein phosphorylation with conformational interpretation using Raman spectroscopy. *Analyst* **2007**, *132* (10), 1053-1060.
18. Ota, C.; Noguchi, S.; Nagatoishi, S.; Tsumoto, K., Assessment of the Protein-Protein Interactions in a Highly Concentrated Antibody Solution by Using Raman Spectroscopy. *Pharmaceutical Research* **2016**, *33* (4), 956-969.
19. Hernandez, B.; Pfluger, F.; Kruglik, S. G.; Ghomi, M., Characteristic Raman lines of phenylalanine analyzed by a multiconformational approach. *Journal of Raman Spectroscopy* **2013**, *44* (6), 827-833.
20. Siamwiza, M. N.; Lord, R. C.; Chen, M. C.; Takamatsu, T.; Harada, I.; Matsuura, H.; Shimanouchi, T., Interpretation of the doublet at 850 and 830 cm⁻¹ in the Raman spectra of tyrosyl residues in proteins and certain model compounds. *Biochemistry* **1975**, *14* (22), 4870-4876.
21. Hernández, B.; Coïc, Y. M.; Pflüger, F.; Kruglik, S. G.; Ghomi, M., All characteristic Raman markers of tyrosine and tyrosinate originate from phenol ring fundamental vibrations. *Journal of Raman Spectroscopy* **2016**, *47* (2), 210-220.
22. Miura, T.; Takeuchi, H.; Harada, I., Characterization of individual tryptophan side chains in proteins using Raman spectroscopy and hydrogen-deuterium exchange kinetics. *Biochemistry* **1988**, *27* (1), 88-94.
23. Takeuchi, H., Raman structural markers of tryptophan and histidine side chains in proteins. *Biopolymers* **2003**, *72* (5), 305-317.
24. Miura, T.; Thomas, G. J., *Subcellular biochemistry, Vol 24, Proteins: Structure, function and engineering*. Plenum Press: New York, 1995.
25. Tsuboi, M.; Suzuki, M.; Overman, S. A.; Thomas, G. J., Intensity of the Polarized Raman Band at 1340-1345 cm⁻¹ As an Indicator of Protein α -Helix Orientation: Application to Pf1 Filamentous Virus. *Biochemistry* **2000**, *39* (10), 2677-2684.
26. Liang, M.; Chen, V. Y.; Chen, H.-L.; Chen, W., A simple and direct isolation of whey components from raw milk by gel filtration chromatography and structural characterization by Fourier transform Raman spectroscopy. *Talanta* **2006**, *69* (5), 1269-1277.
27. Ellepola, S.; Choi, S.-M.; Phillips, D.; Ma, C.-Y., Raman spectroscopic study of rice globulin. *Journal of Cereal Science* **2006**, *43* (1), 85-93.

28. Ashton, L.; Johannessen, C.; Goodacre, R., The importance of protonation in the investigation of protein phosphorylation using raman spectroscopy and raman optical activity. *Analytical Chemistry* **2011**, *83* (20), 7978-7983.
29. Lord, R.; Yu, N.-T., Laser-excited Raman spectroscopy of biomolecules: I. Native lysozyme and its constituent amino acids. *Journal of molecular biology* **1970**, *50* (2), 509-524.
30. Takeuchi, H., UV Raman Markers for Structural Analysis of Aromatic Side Chains in Proteins. *Analytical Sciences* **2011**, *27* (11), 1077-1077.
31. Derbel, N.; Hernandez, B.; Pfluger, F.; Liquier, J.; Geinguenaud, F.; Jaidane, N.; Ben Lakhdar, Z.; Ghomi, M., Vibrational analysis of amino acids and short peptides in hydrated media. I. L-glycine and L-leucine. *J. Phys. Chem. B* **2007**, *111* (6), 1470-1477.
32. Vohník, S.; Tuma, R.; Thomas, G. J.; Hanson, C.; Fuchs, J. A.; Woodward, C., Conformation, stability, and active-site cysteine titrations of Escherichia coli D26A thioredoxin probed by Raman spectroscopy. *Protein science* **1998**, *7* (1), 193-200.
33. Durig, J. R.; Geyer, T. J.; Little, T. S.; Kalasinsky, V. F., Spectra and structure of small ring compounds. 48. Conformational stability of methylcyclobutane from low-frequency Raman data of the gas. *J. Chem. Phys.* **1987**, *86* (2), 545-551.
34. Zhang, D.; Ortiz, C.; Xie, Y.; Davisson, V. J.; Ben-Amotz, D., Detection of the site of phosphorylation in a peptide using Raman spectroscopy and partial least squares discriminant analysis. *Spectrochimica Acta Part A: Molecular and Biomolecular Spectroscopy* **2005**, *61* (3), 471-475.
35. Horne, D. S., A balanced view of casein interactions. *Current Opinion in Colloid & Interface Science* **2017**, *28*, 74-86.
36. Xie, Y.; Jiang, Y.; Ben-Amotz, D., Detection of amino acid and peptide phosphate protonation using Raman spectroscopy. *Analytical biochemistry* **2005**, *343* (2), 223-230.
37. Ashton, L.; Dusting, J.; Imomoh, E.; Balabani, S.; Blanch, E. W., Susceptibility of different proteins to flow-induced conformational changes monitored with Raman spectroscopy. *Biophys. J.* **2010**, *98* (4), 707-714.
38. Morita, S., Perturbation-correlation moving-window two-dimensional correlation spectroscopy. *Applied Spectroscopy*. **2006**, *60* (4), 398.
39. Alaimo, M. H.; Farrell, H. M.; Germann, M. W., Conformational analysis of the hydrophobic peptide α s1-casein (136–196). *Biochimica et biophysica Acta (BBA)-Protein Structure and Molecular Enzymology* **1999**, *1431* (2), 410-420.

For Table of Contents Only

